

# Comparison between Phase Field and ALE Methods to model the Keyhole Digging during Spot Laser Welding

V.Bruyere<sup>1</sup>, C. Touvrey<sup>1\*</sup>, P.Namy<sup>2</sup>

<sup>1</sup>CEA DAM, Valduc, 21120 Is sur Tille

<sup>2</sup>SIMTEC, 8 rue Duployé, Grenoble, 38100 France

[\\*charline.touvrey@cea.fr](mailto:charline.touvrey@cea.fr)

**Abstract:** Nowadays, spot laser welding is a full-fledged part of industrial manufacturing and is routinely used due to its advantages. It generates very located temperature gradients, and therefore, induces small distortions in the pieces. The COMSOL Multiphysics software is used to model the interaction stage of an isolated impact made with a Nd:YAG pulsed laser. The free surface evolution has been precisely described with a moving mesh method (ALE method) by imposing the recoil pressure and the energy deposition as boundary conditions. The results have been compared with those obtained with a fixed mesh method (Phase Field method) for isothermal and thermal cases. A discussion is proposed to choose the more appropriate method to model this problem.

**Keywords:** Welding, ND : YAG pulsed laser, Thermo-hydraulic, ALE, Phase-Field method.

## 1. Introduction

Spot laser welding is used to assemble metal parts by a succession of impacts. This process is routinely used in industrial manufacturing due to its advantages. It generates very located temperature gradients, and therefore, induces small distortions in the pieces. Nonetheless, many welding tests are often performed in order to choose operating parameters leading to a narrow heat affected zone and defect-free joins.

The present paper is focused on the physical phenomena modeling during an isolated impulsion of the laser beam. Before vaporization, the laser beam interacts with an almost flat surface, and the rate of absorbed power (absorptivity) is practically constant. When the vaporization point is reached, the ejected vapor induces a pressure called the recoil pressure. The liquid-gas interface is consequently inserted as a piston and a deep and narrow cavity called the keyhole appears. The formation of the keyhole has several consequences on the laser-matter interaction.

First of all, the trapping of the reflected light into the keyhole provokes a brutal absorptivity increase [1]. The complex mixing of vapor and ambient gas trapped into the keyhole affects then the energy distribution.

Moreover the recoil pressure permanently evolves according to the interface temperature fluctuations [2]. The resulting force particularly depends on the condensation rate compared to the vaporization one [3]. Several models based on adaptations of the Clausius-Clapeyron law aim to quantify the pressure generated at the liquid-gas interface [4-5]. During all the keyhole digging, surface tension forces are opposed to the recoil pressure action. As a consequence, for long interaction duration, an almost stationary state is reached.

Due to the complexity of this multi-physics problem, analytical and semi-analytical approaches are still widely used to study the keyhole dynamics [3-4]. Nevertheless, the progress made in Computational Fluid Dynamics (CFD) enables the feasibility of numerical models. Many authors have adopted Eulerian approaches [6-7] but raise the problem of the gas phase modeling. Indeed, the Mach number in the ejected vapor could reach values up to 0.5. To avoid the problem of the gas modeling, Lagrangian or semi-Lagrangian models have also been proposed to represent more precisely the evolution of the liquid-gas interface position [8-9].

The aim of this study is to compare two kinds of approaches solving free surface problem, in order to choose the more suitable one. As a first approach, the free surface evolution has been precisely described by a moving mesh method (ALE method), by imposing the recoil pressure and the energy deposition as boundary conditions. As a second approach, a fixed mesh method (Phase Field method) has been adopted to take into account the coupling between the gas and the liquid phases. The main phenomena have in this case

been expressed as volume forces, dependent on the Phase Field variable  $\Phi$ .

After a description of the numerical specificities of each method, results are discussed and compared. Concluding remarks are presented at the end.

## 2. Numerical model

All the following equations are computed by means of the finite element software COMSOL Multiphysics V4.3.

As we consider only an isolated impact, an axisymmetric assumption is used. All the calculations have been performed using a well-known material: Ti6Al4V. The properties of this alloy have been previously characterized by many authors [10-11]. The values of the physical parameters used in this study are given in Table 1.

Parameter	Symbol [Unit]	Value [ $T_0, T_{fusion}, T_{vap}$ ]
Ambient temperature	$T_0$ [K]	293.15
Melting point	$T_{fusion}$ [K]	1928
Boiling point	$T_{vap}$ [K]	3600
Melting latent heat	$L_f$ [J.kg <sup>-1</sup> ]	$3.9 \cdot 10^5$
Evaporation latent heat	$L_v$ [J.kg <sup>-1</sup> ]	$8.8 \cdot 10^6$
Thermo-density coefficient	$\beta$ [K <sup>-1</sup> ]	$1 \cdot 10^{-4}$
Surface tension	$\gamma$ [N.m <sup>-1</sup> ]	[-, 1.65, 1.35]
Surface tension variation	$d\gamma / dT$ [N.m <sup>-1</sup> K <sup>-1</sup> ]	$-2.7 \cdot 10^{-4}$
Liquid Viscosity	$\eta$ [Pa.s]	$2.2 \cdot 10^{-3}$
Density	$\rho$ [kg.m <sup>-3</sup> ]	[4500, 4200, 3600]
Heat capacity	$C_p$ [J.kg <sup>-1</sup> .K <sup>-1</sup> ]	[550, 895.2, 895.2]
Heat conductivity	$k$ [W.m <sup>-1</sup> .K <sup>-1</sup> ]	[6, 31.2, 42]

Table 1 – Physical parameters

The laser power has been set to a relatively low level in order to avoid experimental instabilities (especially matter projection), which may cause the process to be non-repeatable. The retained process parameters are presented in Table 2.

Parameter	Symbol [Unit]	Value
Power	$P_{laser}$ [W]	1000
Beam radius	$r_0$ [mm]	0.3
Pulse duration	$t_{interact}$ [ms]	15

Table 2 – Process parameters

### Energy deposition

For both approaches, the interaction between the laser and the metallic vapor still remains a complex problem. Indeed laser beam trapping inside the keyhole is compensated by absorption within the vapor [12].

As a first approach, this part of the problem is simplified. Since the resulting absorptivity of the surface has been previously measured [13] and expecting that the flux deposition is smoothed by the vapor plume, the energy distribution is assumed to be Gaussian-shaped and is consequently modeled by:

$$q_{in} = \frac{P_{laser} \cdot Abs}{\pi r_0^2} e^{-\frac{r^2}{r_0^2}} \quad (1)$$

with  $P_{laser}$  the laser power,  $Abs$  the measured absorptivity as a function of interaction time (from 0.5 to 0.8) and  $r_0$  the beam radius.

### The keyhole digging modeling with a moving mesh method

#### Numerical method

As the computational domain is restricted to the condensed matter (solid and liquid phases), a free surface flow problem has to be solved. Indeed the curvature of the liquid/vapor interface which controls the surface tension effects, evolves during the laser pulse. In order to prevent mesh distortions responsible for poor solution accuracy, an ALE (Arbitrary Lagrangian Eulerian) method is used. At each time step, a steady hyper-elastic problem is solved by propagating the moving boundary displacement throughout the domain to obtain a controlled mesh deformation. The closer the elements are from the interface, the stiffer the virtual hyper-elastic material is to avoid excessive element distortions. Inversely, for the furthest elements, the virtual material is softer to regulate the global deformation. Specific boundary conditions are used to control these mesh displacements. As in

the Lagrangian point of view, the normal component of the mesh velocity ( $\mathbf{u}_{mesh}$ ) at the interface is equal to the normal fluid velocity. For the lateral conditions, the mesh is free to move vertically. Concerning the lowest boundary, the mesh nodes are stationary.

### Thermal problem

In order to evaluate the temperature evolution in the entire domain as a function of time, energy equation is solved in its classical convection/diffusion form:

$$\rho C_p \left( \frac{\partial T}{\partial t} + (\mathbf{u} \cdot \nabla) T \right) = \nabla \cdot (k \nabla T) \quad (2)$$

with  $\rho$  the density,  $C_p$  the heat capacity,  $T$  the temperature,  $\mathbf{u}$  the fluid velocity vector and  $k$  the conductivity.

Melting phase change enthalpy is taken into account by modifying the heat capacity variation with the temperature as:

$$C_p = C_p(T) + \frac{1}{\Delta T \sqrt{\pi}} e^{-\frac{(T-T_{fusion})}{\Delta T^2}} L_f \quad (3)$$

with  $T_{fusion}$  the melting point,  $L_f$  the latent heat of fusion and  $\Delta T$  a numerical parameter set to 50K.

In order to estimate the heat loss, mass flow induced by evaporation has to be evaluated. As proposed by Knight [5], it can be done analytically by considering the re-condensation rate in the Knudsen jump,  $\beta_R$ . The evaporation flux can thus be calculated as follows:

$$q_{evap} = L_v (1 - \beta_R) \sqrt{\frac{M}{2\pi RT}} p_0 e^{\frac{L_v M}{RT_{vap}} \left( 1 - \frac{T_{vap}}{T} \right)} \quad (4)$$

with  $L_v$  the vaporization latent heat,  $p_0$  the pressure at  $T_{vap}$ , the boiling point,  $M$  the molar mass and  $R$  the ideal gas constant.

The energy fluxes applied to the free surface are written as:

$$-\mathbf{n} \cdot (-k \nabla T) = q_{in} - q_{evap} - h(T - T_0) - \varepsilon \sigma_{Boltz} (T^4 - T_0^4) \quad (5)$$

with  $h$  the heat transfer coefficient,  $\varepsilon$  the emissivity,  $\sigma$  the Stefan-Boltzmann constant and  $T_0$  the reference temperature.

For the other boundaries, convective heat flux conditions are considered.

### Fluid modeling

The transport of mass and momentum, governed by the Navier-Stokes equations, is solved in the entire domain for a laminar and transient flow (eq.6). The Boussinesq approximation is assumed to model buoyancy in the weakly compressible fluid flow.

$$\frac{\partial \rho}{\partial t} + \nabla \cdot \rho \mathbf{u} = 0$$

$$\rho \left( \frac{\partial \mathbf{u}}{\partial t} + (\mathbf{u} \cdot \nabla) \mathbf{u} \right) = -\nabla p + \nabla \cdot \left[ \eta (\nabla \mathbf{u} + \nabla \mathbf{u}^T) \right] + \rho \mathbf{g} \beta (T - T_0) \quad (6)$$

with  $p$  the pressure field,  $\eta$  the viscosity,  $\beta$  the thermo-density constant and  $\mathbf{g}$  the gravity vector.

At the liquid gas interface, recoil pressure  $p_{recoil}$  is mainly responsible for the keyhole digging. Normal surface tension forces (Laplace forces) counterbalance the effect of this pressure. Near the irradiated surface, Marangoni effects influence the enlargement of the welding pool. Many approaches can be found in the literature to evaluate the recoil pressure as a function of surface temperature [1]. This non-equilibrium process is often modeled by adjusting the Clausius-Clapeyron law with the re-condensation rate :

$$p_{recoil} = \frac{1 + \beta_R}{2} p_0 e^{\frac{L_v M}{RT_{vap}} \left( 1 - \frac{T_{vap}}{T} \right)} \quad (7)$$

As a first approach, a simplified law will principally be used in this work :

$$p_{recoil} = A e^{-\frac{r^2}{r_0^2}} \quad (8)$$

with  $A$  a numerical parameter.

### The keyhole digging modeling with a fixed mesh method

#### Numerical method

The use of an Eulerian method enables representation of the coupling between the behavior of the gas and the liquid. The Phase Field method (PF) has been retained because it leads to an easier convergence of the problem than the Level Set one [14]. In this case, the two-phase flow dynamics is described by the Cahn-Hilliard equation. The method consists in tracking a diffuse interface separating the

immiscible phases (region where the dimensionless phase field variable  $\Phi$  goes from -1 to 1). Due to the 4<sup>th</sup> order derivative in the Cahn-Hilliard equation, COMSOL solves it with two 2<sup>nd</sup> order equations:

$$\frac{\partial \phi}{\partial t} + \mathbf{u} \cdot \nabla \phi = \nabla \cdot \frac{\kappa \lambda}{\varepsilon^2} \nabla \psi \quad (9)$$

$$\psi = -\nabla \cdot \varepsilon^2 \nabla \phi + (\phi^2 - 1)\phi$$

where  $\mathbf{u}$  is the fluid velocity vector,  $\kappa$  is the mobility,  $\lambda$  is the mixing energy density, and  $\varepsilon$  is the interface thickness parameter.

The mixing energy density and the interface thickness are related to the surface tension coefficient through the relation:

$$\gamma = \frac{2\sqrt{2} \lambda}{3 \varepsilon} \quad (10)$$

The variable  $\chi$  is linked with the mobility  $\kappa$  and with  $\varepsilon$  by the relation  $\chi = \kappa / \varepsilon^2$ . The choice of the phase field parameters ( $\varepsilon$ ,  $\chi$ ) and the mesh size  $h$  is essential to ensure the convergence and the accuracy of the model.

Indeed, for inadequate parameter sets ( $\varepsilon$ ,  $\chi$ , maximum element size  $h$ ), an excessive diffusion can be observed: to obtain acceptable mass losses, the parameter  $\chi$  must be as small as possible. Nevertheless, a high enough value of  $\chi$  must be used to obtain the numerical convergence. The monitoring of the mass conservation in each phase constitutes a good indicator to check the simulation validity (mass losses must be inferior to 3%). The retained parameter set is  $\varepsilon = 2.7e-6m$ ,  $\chi = 1 \text{ m}^{-2}$  and  $h = 3e-6m$ .

To set the normal component of the recoil pressure, the expression (eq.8) is multiplied by the interface normal and by a Dirac function given by the ref [15]. The same method is applied to impose the energy deposition induced by the laser-matter interaction in the liquid/solid phase.

#### Thermal and fluid problem

The energy equation (eq.2) and the Navier-Stokes equations (eq.6) are solved in their classical form like the moving mesh method. All the physical properties are linked to the  $\Phi$  variable with linear relations between the gas and condensed phases.

### 3. Results

#### 3.1 Isothermal Case

In order to compare precisely the two numerical approaches, the fluid problem is first solved in an isothermal regime. Three criteria are used to compare the results: the maximal displacement of the interface at the stationary state, during the transient regime, and the numerical mass losses.

First of all, resulting free surface curvatures are shown at the stationary state in Figure 1 for both approaches.

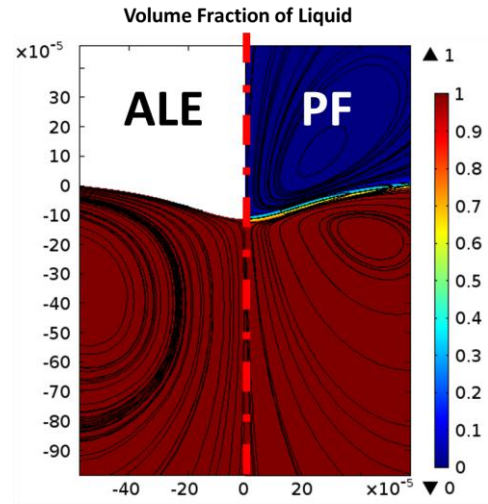


**Figure 1-** Volume fractions of liquid phase obtained at the stationary state with both methods (ALE on the left and Phase Field on the right)

Numerical results are very close concerning the free surface location. An error criterion concerning the maximum of penetration depth is defined as:

$$\varepsilon_{PF/ALE} = 100 \cdot \frac{z_{f=0}^{PF} - z_{f=0}^{ALE}}{\left| \frac{z_{f=0}^{PF} + z_{f=0}^{ALE}}{2} \right|} \quad (11)$$

A value of  $\varepsilon_{PF/ALE} = 0.05\%$  is obtained in this study case.

The interface dynamics is now studied for both approaches. Free surface oscillations at  $r = 0$  are plotted as a function of time in Figure 2. For ALE method, the z-coordinate is directly

obtained; for the PF one, this value is computed for  $\phi = 0$  at  $r = 0$ .

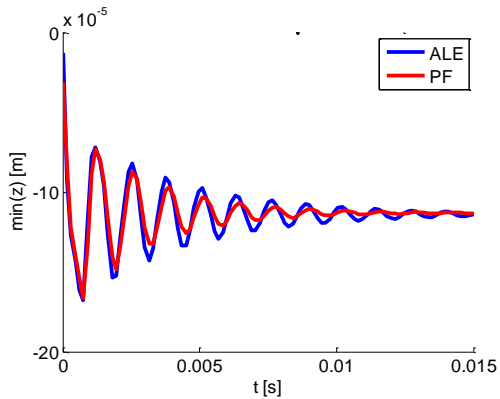


**Figure 2-** Unsteady free surface oscillations as a function of time at  $r = 0$

Again, both methods are in close agreement with each other. The oscillations are however more attenuated because of the interface diffusion with the PF method.

Lastly, the evolution of liquid mass loss as a function of time is compared. It can be seen (Figure 3) that for this case study, both approaches give excellent results concerning the mass conservation (<0.08%).

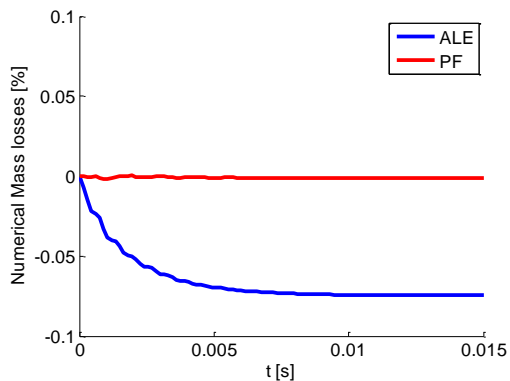


**Figure 3-** Comparison of numerical mass losses between ALE and PF methods

The surface tension implementation in the ALE method and the way to convert surface to volume conditions in the PF theory have thus been validated and can now be used for a more complex problem.

### 3.2 Thermo-hydraulic Cases

Thermal effects are now taken into account in the entire domain. Thermal variations of all physical properties exposed in Table 1 are considered with linear approximations. The solid phase is assumed to behave as a liquid of very high viscosity ( $\eta_{solid} = 1000 \text{ Pa}\cdot\text{s}$ ) when the temperature is below the melting point.

A Gaussian law (eq.8) is used to describe the pressure evolution for each numerical approach with  $A = 4 \cdot 10^4$ . The inward and evaporation fluxes as well as all numerical parameters are also the same for both approaches.

Nevertheless the thermal domain is significantly different. Indeed the computational domain is limited to the condensed phases in the ALE approach; in the phase field one, gas is taken into account and contributes obviously to the thermal exchanges. Moreover, numerical gas properties have been modified (density divided by 10 and viscosity multiplied by 50) to ensure a laminar and incompressible flow :

$$\rho_{gas} = 0.1 \text{ kg}\cdot\text{m}^{-3}, \eta_{gas} = 5 \cdot 10^{-4} \text{ Pa}\cdot\text{s}$$

$$C_{p_{gas}} = 520 \text{ J}/(\text{kg}\cdot\text{K}) \text{ and } k_{gas} = 0.017 \text{ W}/(\text{m}\cdot\text{K}).$$

A first comparison of the temperature field obtained at  $t=8\text{ms}$  is shown in Figure 4.

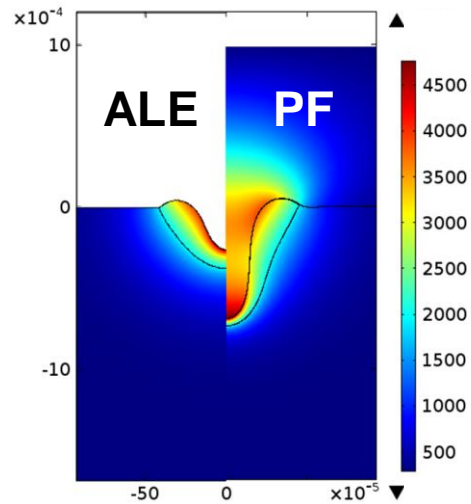


**Figure 4-** Temperature fields for both approaches (ALE on the left and PF on the right) at  $t=8\text{ms}$

Due to the modification of the gas properties in the PF method, the resulting gas velocities are largely underestimated as well as the evaluation



of the energy losses by convection. Temperature in the gas phase is thus wrongly estimated and resulting melted zones shapes are very different for both numerical methods. It highlights the role of the gas media in this thermo-hydraulic modeling.

A parametric study is performed by modifying the gas thermal conductivity (Figure 5).

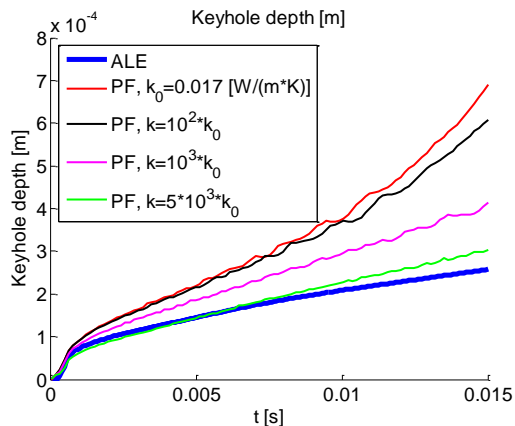


**Figure 5-** Comparison of digging kinetics by varying the gas conductivity in the PF method

By increasing the energy losses by conduction in the gas phase, the liquid phase temperature decreases as well as the keyhole depth (Figure 5). Based on the comparison with the ALE results, the gas conductivity can thus be numerically adjusted to obtain a similar digging kinetics with the PF method.

ALE method gives promising results when the pressure is arbitrarily imposed but reaches its limits when the topology of the interface becomes complex in the case of the pressure/temperature dependence. Nonetheless, surrounding gas is only treated as a boundary condition for fluid (with pressure and surface tension conditions) and thermal (evaporation flux) problems. It permits to easily tackle the complex problem of the not-well-known external media by using analytical simplifications. However, the accuracy of the obtained results can be highly affected and analytical models need to be improved.

The PF method offers a way to model both the gas and liquid/solid domains. It permits to treat complex topology and bubble trapping [14] but due to the complexity of the physical

phenomena happening in this surrounding media, some improvements are necessary to obtain a more representative description.

## 4. Conclusions

Two numerical approaches have been used with COMSOL Multiphysics software to model a three-phase flow problem. They have been compared on a very simple study case without thermal effects. Very satisfying agreements have been found concerning the dynamic and the position of the free surface as well as the mass conservation. After these validations, each approach has been applied to the main thermo-hydraulic problem. ALE method gives promising results when the pressure is arbitrarily imposed but reaches its limits when the topology of the interface becomes complex. Concerning the PF method and because of the complexity of the gas flow, it has been shown that the temperature evolution in the surrounding media can strongly affect the keyhole kinetics. More numerical investigations are necessary to guarantee an accurate modeling of this complex part. Nonetheless, advantages and drawbacks of each method have been clearly identified and developments are in progress for each method to add more physical aspects to this multi-physics modeling.

## 5. References

- [1] R. Fabbro and K. Chouf, Dynamical description of the keyhole in deep penetration laser welding, *Journal of Laser Applications*, **12**, Issue 4, 142-148, (2000).
- [2] Hirano, K., Study on striation generation process during laser cutting of steel, *Ph.D. thesis*, ENSAM (ParisTech) (2012).
- [3] S. I. Anisimov and V. A. Khokhlov, Instabilities in Laser-Matter Interaction, *Boca Raton, FL: CRC*, (1996).
- [4] Semak, W., Bragg, W.D., Damkroger, B., and Kempkas, S., Temporal evolution of the temperature field in the beam interaction zone during laser-material processing, *J. Phys. D: Appl. Phys.*, **32**, 1819-1825 (1999).
- [5] Knight, C. J., Theoretical modeling of rapid surface vaporization with back pressure, *American Institute of Aeronautics and Astronautics*, **17:5**, 19-523 (1979).

- [6] C.L. Chan and J. Mazumder, One dimensional steady state model for damage by vaporization and liquid expulsion due to laser material interaction, *J. phys., D. Appl. Phys.*, **62** (11), 4579-4586 (1987).
- [7] S. Pang, L. Chen, J. Zhou, Y. Yin and T. Chen, A three-dimensional sharp interface model for self-consistent keyhole and weld pool dynamics in deep penetration laser welding, *J. Phys. D: Appl. Phys.*, **44**, 1-15 (2011).
- [8] M. Medale, S. Rabier and C. Xhaard, A thermo-hydraulic numerical model for high energy welding processes, *Rev. Eur. Elements Finis*, **13**, 207-229 (2004).
- [9] X Kong, O Asserin, S Gounand, P Gilles, JM Bergheau and M Medale, 3D finite element simulation of TIG weld pool, *IOP Conf. Series: Materials Science and Engineering*, **33** (2012).
- [10] Boivineau, et al., Thermophysical Properties of Solid and Liquid Ti-6Al-4V (TA6V) Alloy, *Int J Thermophys*, **27**, 507-529 (2006).
- [11] Robert, Y. Simulation numérique du soudage du TA6V par laser YAG impulsif: caractérisation expérimentale et modélisation des aspects thermomécaniques associés à ce procédé, thesis, Mines Paris (ParisTech) (2007).
- [12] C. Y. Ho, M.Y.Wen, Distribution of the intensity absorbed by the keyhole wall in laser processing, *J. Mater. Process. Technol.* **145**, 303-310 (2004).
- [13] Touvrety-Xhaard, C., Etude thermo-hydraulique du soudage impulsif de l'alliage TA6V. Ph.D. thesis, Université de Provence (Aix-Marseille I) (2006).
- [14] Touvrety, C. and Namy, P. Formation of Porosities during Sport Laser Welding of Tantalum, *Proceedings of COMSOL European Conference* (2011)
- [15] Boiling water, *COMSOL Tutorial*.